Published in final edited form as:

Sci Immunol. 2019 March 15; 4(33): . doi:10.1126/sciimmunol.aav1263.

CD4 T cell sphingosine 1-phosphate receptor (S1PR)1 and S1PR4 and endothelial S1PR2 regulate afferent lymphatic migration

Yanbao Xiong[1,2,9], **Wenji Piao**[1,2,9], **C. Colin Brinkman**[2], **Lushen Li**[1,2], **Joseph M. Kulinski**[3], **Ana Olivera**[3], **Andreane Cartier**[4,5], **Timothy Hla**[4,5], **Keli L. Hippen**[6], **Bruce R. Blazar**[6], **Susan R. Schwab**[7], **Jonathan S. Bromberg**[1,2,8,*]

[1]Department of Surgery, University of Maryland School of Medicine, Baltimore, MD 21201

[2]Center for Vascular and Inflammatory Diseases, University of Maryland School of Medicine, Baltimore, MD 21201

[3]Mast Cell Biology Section, Laboratory of Allergic Diseases, NIAID, NIH Bethesda, MD 20892

[4]Vascular Biology Program, Boston Children's Hospital, Boston, MA 20115

[5]Department of Surgery, Harvard Medical School, Boston, MA 20115

[6]University of Minnesota Cancer Center and the Department of Pediatrics, Division of Blood and Marrow Transplantation, University of Minnesota, Minneapolis, MN 55455

[7]Skirball Institute of Biomolecular Medicine, New York University School of Medicine, New York, NY 10016

[8]Department of Microbiology and Immunology, University of Maryland School of Medicine, Baltimore, MD 21201

[9]These authors contributed equally to this work.

Abstract

Sphingosine 1-phosphate (S1P) and S1P receptors (S1PR) regulate migration of lymphocytes out of thymus to blood and lymph nodes (LN) to efferent lymph, while their role in other tissue sites is not known. Here we investigated the question of how these molecules regulate leukocyte migration from tissues through afferent lymphatics to draining lymph node (dLN). S1P, but not other chemokines, selectively enhanced human and murine CD4 T cell migration across lymphatic endothelial cells (LEC). T cell S1PR1 and S1PR4, and LEC S1PR2, were required for migration across LEC and into lymphatic vessels and dLN. S1PR1 and S1PR4 differentially regulated T cell motility and VCAM-1 binding. S1PR2 regulated LEC layer structure, permeability and expression of the junction molecules VE-cadherin, occludin and zonulin-1 through the ERK pathway. S1PR2

[*]***Correspondence:*** Jonathan S. Bromberg, Department of Surgery, University of Maryland School of Medicine, 22 S. Greene Street, S8B06, Baltimore, MD 21201, jbromberg@som.umaryland.edu, Phone: 410 328 0008, Fax: 410 328 6343 .

Author contributions: Y.X. and J.S.B. designed the research, planned and analyzed the experiments, wrote the manuscript; Y.X., W.P., C.C.B., and L.L. performed the experiments; J.M.K. and A.O. provided S1PR2$^{-/-}$, S1PR4$^{-/-}$, Sphk1$^{-/-}$, Sphk2$^{-/-}$ mice; A.C. and T.H. provided S1PR1$^{-/-}$, S1PR1-Tg, S1PR1^{S5A} mice; K.L.H. and B.R.B. provided human T cells; S.R.S. provided S1PR1$^{-/-}$ mice; all collaborators made important suggestions on experimental design and manuscript review.

Competing interests: The authors declare no competing interests.

facilitated T cell transcellular migration through VCAM-1 expression and recruitment of T cells to LEC migration sites. These results demonstrated distinct roles for S1PRs in co-modulating T cell and LEC functions in migration and suggest new levels of regulation of leukocytes and endothelial cells during homeostasis and immunity.

Introduction

S1P controls T cell migration from thymus to the blood across microvascular endothelium, and egress from lymph node (LN) to lymphatics across lymphatic endothelium. These activities are primarily mediated by S1P receptor 1 (S1PR1) (1). The S1P/S1PR1 axis acts on T cells, as a signal to leave the LN (2, 3), and on endothelial cells to alter barrier function (4, 5). While less is known about use of S1P for migration in peripheral tissues, we previously showed that S1P/S1PR1 acted as a stop signal for T cells, but the effects of S1P gradients were not evaluated (6).

S1P regulates endothelial cell homeostasis (7–10) and barrier function (11, 12) *)*, which are important for leukocyte trafficking. Therefore, unlike the responses to traditional chemokines where only leukocytes express the cognate receptors, both cell types express one or more receptors for S1P, making it possible for S1P-driven migration to be regulated differently. The variability in receptor expression and utilization suggests additional levels of complexity in the regulation of migration.

There are five G protein-coupled receptor (GPCR) S1PRs: S1PR1, 3–5 are linked to G_i, while S1PR2 preferentially signals via $G_{12/13}$ (13). Pertussis toxin (PTX) inhibits S1PR1, 3–5 through G_i, but does not inhibit $G_{12/13}$ or S1PR2. The nonspecific S1PR antagonist FTY720 binds S1PR1, 3–5 with much higher affinity than S1PR2 and has no inhibitory effects on S1PR2 (4). S1PRs regulate diverse leukocyte activities. S1PR1 directs B cells to the splenic marginal zone (14), and controls immature B cell egress from bone marrow (15). S1PR1 promotes human B cell migration, which is in turn modulated by S1PR4 and S1PR2 (16). S1P regulates macrophage entry and egress from LN (17). Mature DC migrate to S1P (18), and CD69 modulates S1P-induced migration from skin to draining LN (dLN) (19). S1PRs regulate ILC2 entrance into lymphatic vessels and egress from LN (20).

Here we looked at the roles of S1PRs in T cells and in LECs and showed that T cells responded to S1P gradients through S1PR1 and S1PR4 to migrate across afferent LEC. S1PR1 and S1PR4 had distinct roles in T cell motility and binding to VCAM-1. The T cell-LEC interaction engaged LEC S1PR2-dependent processes to promote T cell transcellular migration, which was distinct from chemokine driven migration. S1PR2 signaled through ERK to regulate lymphatic permeability and LEC surface and junction proteins. These results demonstrated trans-lymphatic endothelial migration (TEM) relies on several receptors with integrated process of both T cell and LEC responses to a common ligand.

Results

S1P selectively promotes trans-endothelial migration

We previously established a TEM assay in which primary murine LEC or the mouse endothelial cell line SVEC were seeded on the lower surface of a transwell insert (designated as iLEC or iSVEC) (Fig. S1A), allowing establishment of junctions and polarity (21). Leukocytes loaded in the upper chamber migrated across the LEC layer from the basal (or abluminal) to the apical (or luminal) direction. Migration only proceeded in the basal to apical direction, recapitulating directional migration in vivo.

Only low numbers of T cells migrated across transwell plastic membranes to S1P (Fig. S1B) (22). Using the TEM model, we found far more CD4 T cells migrated across primary LEC and the SVEC line in a dose-dependent fashion (Fig. 1A–C). However, CD4 T cell TEM to CCL19 or other chemokines and cytokines was not enhanced compared to plastic (Fig. 1A–B, Fig. S1C–H). LEC promoted migration toward S1P of various mouse CD4 T cell subsets, including memory (Tmem) and activated effector cells (Teff) (Fig. S1I–K). Human effector T cells and Treg also migrated more across human iLEC than plastic in response to S1P, but not CCL19 (Fig. 1D, Fig. S1L–M). These results suggested that S1P-driven TEM involved actively stimulated interactions on both T cells and LEC, in contrast to chemokine driven migration where ligands engaged cognate receptors only on T cells.

When DC cross afferent LEC, the interaction results in CCL21 secretion by the LEC to enhance entry into the lymphatics (23–25). In our model, CD4 T cell TEM to CCL19 was significantly inhibited by anti-CCL21 (Fig. 1E), suggesting that LEC secreted CCL21 in response to CD4 T cells. Indeed, primary LEC and SVEC, along with afferent lymphatics, all constitutively expressed CCL21 (Fig. S2A–B). In contrast, S1P-driven migration was not inhibited by anti-CCL21, suggesting migration mechanisms and their regulation by LEC were distinct from CCL21-driven migration (Fig. 1E).

S1P may stimulate LEC to express other chemotactic molecules (26). SVEC were treated with S1P and supernatants collected separately from upper and lower chambers. These supernatants were applied to the upper and lower chambers, respectively, of a second TEM assay. Anti-S1P mAb was also added to supernatants to exclude an effect of the S1P added to the primary cultures. Neither upper chamber nor lower chamber supernatants enhanced migration (Fig. S2C). To determine if S1P induced chemotactic factors that remained bound to the endothelial cells, SVEC were pretreated with S1P, washed, and T cells added. S1P pretreatment of SVEC slightly, although not significantly, enhanced migration (Fig. S2D). Lastly, anti-S1P added to the upper chamber inhibited TEM in a dose-dependent fashion (Fig. 1F). Together, these results excluded the possibility that enhanced T cell migration was due to additional chemotactic factors produced by LEC after S1P stimulation.

Fluorescence microscopy was used to monitor T cell real-time movements across LEC layers. The velocity and transit times of migration toward S1P and CCL19 were similar (Fig. 1G–H), showing that once CD4 T cells engaged LEC in the presence of S1P, the T-LEC interactions resulted in similar kinetics as for chemokine-driven T cell migration.

Transendothelial migration toward sphingosine 1-phosphate is chemotactic, chemokinetic and responsive to flow and inflammation

S1P loaded in the lower or both chambers, but not the upper chamber alone, resulted in enhanced TEM (Fig. 2A). Thus, S1P-driven TEM was chemokinetic and chemotactic, but not chemorepulsive (Fig. 2A). Real-time migration over LEC was measured under these conditions (Fig. 2B). T cells migrated with the same displacement for all groups, but migrated with higher velocities when S1P was in the lower chamber (chemotaxis) or both chambers (chemokinesis) (Fig. 2C–D). S1P induced a change in the velocity distribution so more CD4 T cells had higher velocities (Fig. 2E). These results suggested that chemotactic and chemokinetic responses engaged similar migration mechanisms.

Trans-lymphatic fluid flow affects the phenotype and function of lymphatic monolayers (27, 28). We previously mimicked interstitial fluid flow by creating a pressure differential of 0.8–0.9 cm H_2O that resulted in an average flow 15.8 μl/h (27, 28). The flow enhanced TEM toward S1P and CCL19 (Fig. 2F) suggesting that flow characteristics for both ligands were similar.

VLA-4-VCAM-1 interactions are important for chemokine-driven TEM, and migration could be partly inhibited with blocking mAbs (27). VCAM-1 expression on LEC was enhanced by TNFα, which increased TEM (6) (29). Similarly, TNFα enhanced S1P-driven TEM (Fig. 2G). Blocking anti-VLA-4 or anti-VCAM-1 mAbs partly inhibited migration (Fig. 2G), suggesting VLA-4-VCAM-1 dependent and independent TEM, as noted for chemokine driven migration. Overall, these results showed that S1P-driven migration shared several characteristics with chemokine driven migration.

After inflammation induced by LPS treatment of footpads, CD4 T cell migration into dLN was increased (Fig. 2H), and migration was blocked by anti-VCAM-1 mAbs (Fig. 2I). Thus, CD4 T cell homing into dLN under both homeostatic and inflammatory conditions was dependent on VLA-4/VCAM-1 interactions and S1P (Fig. 4B–C).

Expression of S1PR1 and S1PR4 on CD4 T cells is required for migration into lymphatics

S1PR1 is linked to G_i, S1PR3–5 are linked also to G_q, and S1PR2 is linked to $G_{12/13}$, resulting in differential sensitivity to receptor and G protein antagonists (13). RT-PCR (Fig. S2E) and western blotting (Fig. S2F) confirmed that primary LEC and SVEC expressed S1PR1 and S1PR2 (30). Naïve CD4 T cells, Teff and Tmem expressed S1PR1 and S1PR4 (Fig. S2E, S2G-I) (13, 31).

G_i-coupled S1PR1, 3–5 are inhibited by PTX, and FTY720 induces functional antagonism of S1PR1 but not S1PR2. CD4 T cells pretreated with PTX or FTY720 had significantly decreased migration (Fig. 3A, Fig. S3A), suggesting that T cells use S1PR1 and/or S1PR4 for TEM. Using specific pharmacologic inhibitors, treatment of T cells with a reversible S1PR1 antagonist (32), and an irreversible S1PR4 antagonist (33), inhibited migration (Fig. 3B–C, Fig. S3B–C). These inhibitors did not alter T cell viability (Fig. S3D). We concluded that T cells used both S1PR1 and S1PR4 to respond to S1P-driven TEM.

To confirm these findings, tamoxifen induced S1PR1$^{-/-}$ conditional deletion and S1PR4$^{-/-}$ germline deletion T cells were assessed. Deletion of either receptor resulted in poor migration responses to S1P, while migration to CCL19 remained intact (Fig. 3D–E). The S1PR1 and S1PR4 antagonists were also inactive on the receptor deficient cells. These results confirmed the findings with the pharmacologic inhibitors and ruled out off-target or nonspecific effects. T cells from S1PR1-Tg (Fig. 3F) or S5A (Fig. 3G) mice, in which there were higher levels of cell surface S1PR1 (7, 34) *)*, had enhanced CD4 T cell migration toward S1P, but not CCL19 (Fig. 3F–G), showing the critical function of S1PR1 in TEM. T cells were pretreated with antagonists and migration to S1P loaded into the lower or both chambers was assessed. The results showed that both S1PR1 and S1PR4 antagonists inhibited chemotaxis and chemokinesis (Fig. 3H). Thus, S1PR1 and S1PR4 regulated both types of movements and were additive for chemotaxis.

To assess pharmacologic blockade in vivo, T cells were pretreated with inhibitors, transferred to hind footpads, and migration to popliteal dLN assessed. The S1PR4 antagonist inhibited migration (Fig. 3I), while there was a trend for migration inhibition with the S1PR1 antagonist (Fig. 3J); lack of significance was likely due to the reversibility of this compound. The combination of S1PR1 plus S1PR4 antagonists inhibited migration more completely (Fig. S3E). S1PR1$^{-/-}$ and S1PR4$^{-/-}$ T cells migrated less to dLN compared to wild type CD4 T cells (Fig. 3K–L). In contrast, S1PR1 S5A CD4 T cells migrated more into dLN compared to wild type (Fig. 3M).

Tmem and Teff are the major subsets that migrate from tissues into dLN through afferent lymphatics (35, 36). Similar to naïve T cells, pretreatment of Teff (Fig. 3N) and Tmem (Fig. 3O) with S1PR1 and S1PR4 antagonists inhibited migration in vitro. S1PR1$^{-/-}$ Teff (Fig. 3P) and Tmem (Fig. 3Q) and S1PR4$^{-/-}$ Teff (Fig. 3R) and Tmem (Fig. 3S) migrated less. In vivo, S1PR1 (Fig. 3T) and S1PR4 (Fig. 3U) antagonists inhibited Teff migration to dLN. Overall, S1PR1 and S1PR4 were required for homing of various T cell subsets into dLN through afferent lymphatics.

S1P gradients and expression of S1PR2 on LEC are required for trans-endothelial migration

Whole mount staining of ear pinnae showed S1P was present around the afferent lymphatics (Fig. 4A), revealing proximity of S1P to the lymphatics and that S1P distribution appears to establish a gradient. S1P-regulated chemotaxis was confirmed since anti-S1P mAb administered to the footpad inhibited migration into dLN under homeostatic and inflammatory conditions (Fig. 4B–C). T cells migrated less into dLN of Sphk1$^{-/-}$ and Sphk2$^{-/-}$ mice (Fig. 4D), deficient in S1P production (37). Ear whole mounts showed S1P expression was diminished around afferent lymphatics of Sphk1$^{-/-}$ and Sphk2$^{-/-}$ strains (Fig. S3F). Lyve-1 and CCL21 expression in Sphk1$^{-/-}$ and Sphk2$^{-/-}$ lymphatics did not differ from wild type (Fig. S3F), and the morphology and density of lymphatic vessels appeared normal. Pre-incubation of anti-S1P mAb with S1P abolished staining showing additional specificity (Fig. S3G). Thus, morphologic alterations did not account for changes in migration.

Treatment of LEC with PTX or FTY720 did not inhibit migration (Fig. 3A, Fig. S3A), suggesting use of S1PR2 instead of S1PR1. Pretreatment of LEC, but not naive T cells, with the S1PR2 antagonist specifically decreased migration (Fig. 4E, Fig. S3H). Teff and Tmem migration were inhibited by LEC pretreatment with S1PR2 inhibitor (Fig. 4F and 4G). LEC pretreatment with S1PR4 antagonist did not inhibit migration (Fig. 3C, Fig. S3C), and S1PR2$^{-/-}$ CD4 T cell migration was not inhibited toward S1P or CCL19 (Fig. S3I), showing cell specificity for receptor blockade. It was not possible to treat T cells or LEC alone with the S1PR1 inhibitor since it was reversible (32). However, S1PR2 but not S1PR1 knockdown of SVEC (Fig. S3J–K) resulted in decreased TEM toward S1P but not CCL19 (Fig. 4H, Fig. S3L).

To assess blockade in vivo, pretreatment of footpads, but not T cells, with S1PR2 antagonist inhibited naïve and effector T cell migration (Fig. 4I–J, Fig. S3M). To validate these findings for endogenous T cells, we administered anti-CD62L i.v. to prevent leukocyte entrance into LN through blood, and the S1PR2 antagonist was injected into the footpad (27, 29). Analysis of the dLN showed that S1PR2 antagonist reduced endogenous CD4^{+}CD44^{hi} memory and CD4^{+}CD69^{+} activated T cell homing (Fig. 4K). Wild type CD4 T cells migrated less in S1PR2$^{-/-}$ (Fig. 4D), while S1PR2$^{-/-}$ CD4 T cells migrated the same as wild type (Fig. S3N). Ear whole mounts showed S1P, Lyve-1, CCL21, morphology and lymphatic density were normal for S1PR2$^{-/-}$ afferent lymphatics (Fig. S3F). Overall, the results demonstrated that LEC S1PR2 regulated in vitro and in vivo migration of multiple CD4 T cell subsets.

S1PRs and CCR7 have distinct roles in trans-endothelial migration

Combined treatments of LEC with S1PR2 antagonist and T cells with S1PR1 and S1PR4 antagonists almost completely blocked naïve T cell (Fig. 4L) and Teff (Fig. 4M) migration in vitro. T cell migration into dLN was completely blocked with the combination of antagonists in vivo (Fig. 4N). CCR7 is a potent regulator for T cell afferent lymphatic migration (6). To test for an interaction or preference for S1PRs and CCR7, CD4 T cell migration to S1P plus CCL19 was assessed. When both were combined, there was an additive effect (Fig. 4O). S1PR1, S1PR2 and/or S1PR4 antagonists blocked migration, and to a greater extent than the component contributed by S1P alone (Fig. 4O). Anti-CCR7 blocked CD4 T cell migration toward S1P plus CCL19 (Fig. 4O), and CD4 T cell homing into dLN (Fig. S4A). These results suggested that S1PRs and CCR7 were independently required by CD4 T cells for TEM, although CCR7 appeared more potent compared to the various S1PRs. None of the S1PR antagonists inhibited TEM driven by CCL19 (Fig. S4B, excluding off-target events and cross-talk among different GPCR.

To distinguish why different receptors were required for TEM, S1P or CCL19 alone or combined were added to the migration assays, and antagonists added at various times. The S1PR antagonists only blocked migration when added early, while anti-CCR7 blocked migration at both early and late times, and this was true for single or combined ligands (Fig. 4P, Fig. S4C–D). These findings suggested that S1P-S1PRs were required for early migration events and interactions between T cells and LEC, while CCL19-CCR7 were required for later interactions.

S1P-S1PRs regulate afferent lymphatic entry

Immunohistochemistry of the dLN showed CFSE-labeled, transferred CD4 T cells had the same distribution patterns among vehicle, S1PR1, S1PR4 and S1PR2 antagonist treated groups (Fig. S5A), and S1PR2 antagonist did not change LN architecture (Fig. S5B). This suggested that inhibitors prevented migration across lymphatic endothelium and into lymphatic vessels, rather than block downstream events, such as entry into the subcapsular space or dLN parenchyma.

To verify that S1PRs regulated CD4 T cell migration across lymphatic endothelium in vivo, CD4 T cells treated with antagonists were transferred into pinnae. Whole mount staining showed the S1PR4 antagonist inhibited CD4 T cell migration nearby and into the afferent lymphatic vessel lumens (Fig. 5A, Fig. S5C). S1PR4$^{-/-}$ CD4 T cells migrated less efficiently nearby or into lymphatics (Fig. 5B, Fig. S5D). S1PR1 antagonist prevented migration nearby or into the afferent lymphatics (Fig. 5C, Fig. S5E). In contrast, S1PR1Tg and S1PR1 S5A CD4 T cells migrated into afferent lymphatics more rapidly and completely, so only 2 hours after transfer there was already significant migration into vessels (Fig. 5D–E). CD4 T cells failed to migrate into vessels in ears pretreated with anti-S1P mAb or S1PR2 antagonist (Fig. 5F–G). Wild type CD4 T cells failed to enter lymphatics of S1PR2$^{-/-}$ recipients (Fig. 5H). The role of CCR7 in afferent lymphatic distribution was also assessed: anti-CCR7 treatment of the pinnae prevented T cell migration nearby or into the afferent lymphatics (Fig.S5F). These results demonstrated the locus of S1P-S1PR as TEM and entry into the vessel.

S1PR2 signals through ERK to regulate LEC permeability and junction molecule expression

S1PR2 activates the MAPKs p38 and JNK in blood vascular endothelial cells (30, 38). Similarly, S1P induced phosphorylation of p38, JNK, and ERK1/2 in LEC (Fig. 6A). S1PR2, but not S1PR1, antagonism specifically inhibited phosphorylation (Fig. 6A). Endogenous S1P synthesis also regulates LEC (39), and the Sphk inhibitor (Sphki) decreased ERK phosphorylation in untreated cells, while p-ERK was restored by exogenous S1P (Fig. 6B). Together, these results showed that exogenous or endogenous S1P stimulated LEC S1PR2 and MAPKs.

To determine if the signaling regulated LEC structure and function, cell layers were treated with S1P and/or inhibitors, and layer permeability assessed by dye transport. The S1PR2 antagonist decreased permeability, while exogenous S1P, anti-S1P or FTY720 did not (Fig. 6C–E). The ERK inhibitor also decreased permeability (Fig. 6F). The antagonists did not alter LEC viability (Fig. S5G). The S1PR2 antagonist inhibited lymphatic dye transport from tissues into dLN (Fig. 6G). Thus, S1PR2 and ERK regulate LEC permeability.

The permeability changes suggested S1P alters cell junctions (39). Overlapping flaps at endothelial boarders of initial lymphatics are connected by discontinuous button-like junctions, comprised of VE-cadherin and other junction-associated proteins (40); DCs penetrate into afferent lymphatics through the portals between button junctions (41). To assess these junctions, pinnae or LEC were treated with inhibitors, and the effects on

junctional proteins and structures measured. S1PR2 inhibition resulted in increased numbers of VE-cadherin positive buttons (Fig. 6H), along with increased expression of the junction molecules occludin and zonulin-1 (ZO-1) (Fig. 6I–J). In S1PR2$^{-/-}$ pinnae the afferent lymphatic terminals expressed more VE-cadherin and buttons (Fig. 6K). The S1PR2 antagonist and ERK inhibitor, but not the other S1PR antagonists, increased VE-cadherin, ZO-1, and occludin expression (Fig. 7A–C). Together, these results suggested that S1P-S1PR2 triggered ERK signaling thereby altering LEC layer permeability through junction molecule expression.

S1PR2 signals through ERK to regulate transcellular TEM

Since S1P-S1PR2-ERK regulated permeability and junction structure, we next determined how this affected TEM. The ERK inhibitor blocked TEM (Fig. 7D). We previously showed S1PR2 signaling in HUVECs involved Rho or Rho-associated protein kinase (ROCK) and PTEN (38), and regulated endothelial permeability and junction integrity. This additional pathway was active here as Rho and ROCK inhibitors decreased TEM (Fig. 7E). Together, these results suggested that S1P-S1PR2 triggered ERK signaling thereby altering LEC layer permeability through junction molecule expression, which regulated TEM.

Leukocytes cross endothelium via paracellular and transcellular routes, which depend on endothelial cell junction structures (42, 43). We previously demonstrated CCL19-driven TEM used both routes equally (6). Here we found that the transcellular position was preferentially engaged for S1P-driven T cell migration (Fig. 7F.i). The S1PR1, S1PR2, and S1PR4 antagonists not only inhibited overall migration, but each also reduced the percentage of transcellular migration (Fig. 7F.ii). Anti-VCAM-1 and Rho and ROCK inhibitor treatments also reduced the percentage of transcellular migration (Fig. 7F.iii, Fig. S5H), while the ERK inhibitor did not change the preference for migration route (Fig. S5H). Thus, changes in permeability and junction molecule expression are reflected in the physical pathways for TEM. Overall, S1P-S1PR2 signaling recruited all these molecules, with preferences for use of several in transcellular migration.

S1PR2 regulates endothelial expression of, and S1PR1 and S1PR4 regulate T cell binding to, VCAM-1

As noted above, S1P-mediated TEM was dependent on VCAM-1-VLA-4 (Fig. 2G). S1PR2 upregulates VCAM-1 expression on blood vascular endothelial cells (44). To investigate S1PRs regulation of VCAM-1 expression, we noted VCAM-1 expression on SVEC (Fig. 8A–B, Fig. S6A–B) and primary LEC (Fig. S6C–D) was downregulated by S1PR2 but not S1PR1 inhibitor, without affecting other receptors such as Lyve-1. ERK inhibitor U0126 decreased VCAM-1 expression (Fig. 8A–B). VCAM-1 expression was decreased by Sphki inhibition of endogenous S1P synthesis (Fig. 8C), and partially restored by exogenous S1P. VCAM-1 on the LEC surrounded and facilitated T cell transmigration (45), and T cells did not express VCAM-1 (Fig. S6E). The S1PR2 antagonist and the ERK inhibitor both inhibited VCAM-1 expression and recruitment around the T cells (Fig. 8D–E). The S1PR2 antagonist also inhibited VCAM-1 expression in vivo (Fig. 8F). Like the S1PR2 inhibitor, the ERK inhibitor decreased CD4 T cell migration (Fig. 6O). Together, these results confirmed S1P-S1PR2-ERK regulation of VCAM-1 expression by LEC, a tight association

between migrating T cells and LEC VCAM-1, and the importance of VLA-4-VCAM-1 in TEM.

It has been reported that VCAM-1 forms a transmigratory cup to direct leukocyte TEM (46). To further investigate the role of T cell-VCAM-1 interactions for migration, transwell inserts were coated with VCAM-1-Ig without LEC, and T cell migration to S1P and VCAM-1 assessed. Both S1P and VCAM-1 promoted T cell migration in an additive manner (Fig. 8G). The S1PR4 but not the S1PR1 antagonist prevented S1P plus VCAM-1-driven migration (Fig. 8G). To verify the specificity, anti-VLA-4 treatment also blocked T cell migration (Fig. S6F). This regulation was highly specific since ICAM-1-Ig promoted CCL19 but not S1P-driven migration (Fig. S6G). Real-time imaging across LEC showed S1PR1 antagonism reduced T cell migration distances, but not migration velocities, although the very highest velocities were inhibited; while S1PR4 antagonism decreased both distances and velocities (Fig. 7H). The results suggested that the specific role of S1PR4 was to regulate the interaction of T cells with VCAM-1. Since the S1PR1 antagonist actually increased migration to a small extent, the results suggested S1PR1 may regulate adhesion and/or release of the T cell from adhesion to permit continued migration.

Discussion

T cell S1PR1 and S1PR4 plus LEC S1PR2 were necessary for TEM. S1P gradients not only acted as chemotactic signals for T cells, but also regulated LEC to facilitate T cell TEM. This suggested active co-engagement of T cells and LEC due to S1P signaling. In contrast to chemokines, S1P-driven migration required LEC, was chemotactic and chemokinetic, preferentially utilized transcellular routes, but was not facilitated by LEC-derived CCL21. Since LEC-derived CCL21 is necessary for DC tissue egress (23, 47), it was possible that S1PRs mobilized an intracellular CCL21 pool that anti-CCL21 failed to target this pool. The preferential use of transcellular migration may support such a hypothesis. S1PR2 regulated downstream signal p38, ERK and JNK activation, endothelial permeability, junction proteins and VCAM-1 expression and distribution, LEC buttons, and transcellular TEM. S1P-driven migration was similar to chemokines for use of VCAM-1-VLA-4, responsiveness to fluid flow, and modulation by inflammation.

Many investigations of S1PR1 in thymus, blood and LN, demonstrating that it controls T cell trafficking at multiple stages of T cell development and responses (1, 2, 13). The present findings add to the roles played by S1P and S1PRs in T cell migration. S1PR1 and S1PR4 had similar magnitudes of effect on migration or migration inhibition, were required early in the migration response (, regulated transcellular migration, regulated chemotaxis and chemokinesis, and altered T cell positions around lymphatic vessels and lumens. Their major functional differences were in T cell motility and interaction with VCAM-1. Enforced surface expression of S1PR1 showed that S1PR1 promoted CD4 T cell afferent lymphatic TEM, while down modulation prevented this. A recent study of human T cell migration across plastic showed different T cell subsets used both S1PR1 and S1PR2 (48), suggesting different S1PRs expression by human and murine T cells. In our previous report (6), high local concentrations of S1P in inflammation acted as a stop signal for TEM, by down modulation of S1PRs and possibly altering the S1P gradient. The ability of S1P to stimulate

chemokinesis suggests tissue egress may still occur despite increased local S1P concentrations.

S1P regulates important aspects of endothelial cells, including blood vascular endothelial cell spreading, maturation and stabilization, and barrier integrity (49), independent of VE-cadherin (49) and through S1PR1 and S1PR3 (49). Less is known about S1P and S1PRs in regulating LEC. We demonstrated S1PR2 regulated LEC and lymphatic barrier permeability and junction molecules expression. S1PR1 did not play the same role, although S1PR1 can regulate blood endothelial cell permeability and mobility (49), so S1PR1 might have complementary roles to S1PR2 in other circumstances. Exogenous S1P did not change basal barrier function, suggesting endogenous S1P maintained tonic barrier integrity, which was inhibited by S1PR2 blockade. S1P-S1PR2 induced ERK activation and regulated VCAM-1 and VE-cadherin, zonulin, and occludin expression. Inhibition of S1PR2 altered VCAM-1 and VE-cadherin expression, along with changes in the density and distribution of the button and zipper endothelial junctions, and changes in the interaction of CD4 T cells and LEC during TEM. These findings suggested that S1P-S1PR2-ERK regulated junctional and adhesion molecule expression, distribution and function, which controlled LEC permeability and transcellular TEM. The results also suggested a simultaneous role for Rho and ROCK, which are regulated by S1PR2 in blood endothelial cells (38).

Paracellular and transcellular TEM involve dissimilar mechanisms, although both rely on recruitment of membrane from the lateral border recycling compartment (42, 43). During paracellular migration, VE-cadherin moves away from the migration site (42). S1PR2 decreases while its antagonist increases VE-cadherin on HUVEC (38). We found S1PR2 and ERK antagonists increased VE-cadherin expression and reduced migration, suggesting VE-cadherin was involved in both migration routes. We previously demonstrated CCL19-driven migration across LEC used both routes (6); and FTY720 caused preferentially transcellular migration, suggesting S1PRs differentially regulate the two pathways. We found transcellular migration was preferentially engaged by S1P-S1PR2, which may explain why S1P but not CCL19 promoted T cell-LEC interactions for enhanced migration. Anti-VCAM-1 mAbs and ROCK and Rho inhibitors reduced the proportion of T cells migrating through the transcellular route toward S1P, while ERK inhibitor did not significantly change this proportion. Thus, S1P-S1PR2 signaling recruited all these molecules, with preferences for use of some in transcellular migration.

Several receptors are needed for TEM and distinct roles and functions were defined. The S1PR1 inhibitor increased migration through VCAM-1, suggesting S1PR1 regulated binding and/or release of T cells from adhesion. In contrast, the S1PR4 inhibitor blocked migration, so S1PR4 is responsible for migration through VCAM-1. S1PR1 regulated migration distances but not velocities, while S1PR4 regulated both distances and velocities. There was sequential use of S1PRs and CCR7: S1PRs were engaged early while CCR7 was engaged later. LEC promoted S1P but not CCL19-driven migration; and T cells migrated toward CCL19 equally through paracellular and transcellular routes, whereas S1P-driven migration preferentially employed the transcellular route. These observations suggest S1PRs mediated T cell-LEC interactions and initiated T cell transcellular migration at early time points that could not be reversed by S1PRs antagonists. In contrast, CCR7-driven migration depended

on the CCL19 gradient and could be blocked at later times. Our findings suggest new areas requiring more investigation. The precise T cell-LEC interactions will require more definition of the receptors and ligands involved at the cell surfaces and events that determine cytoskeletal and membrane movements. Such investigations will likely shed more light on how and why multiple receptors must be used simultaneously for migration. The pathways engaged by S1PR1, S1PR4, and CCR7 for T cell movements to and across LEC will require investigation at higher magnification, to visualize subcellular and molecular movements. It will be even more challenging to confirm in vitro observations with in vivo models, and to determine if efferent and afferent lymphatics function similarly or not, or if other lymphatics beds have unique responses (50). The intercellular interactions seem dependent on each other, so analyses will have to account for the complexity of complementary T cell and endothelial cell responses, particularly in teasing out the decision of both cells to use paracellular versus transcellular migration pathways.

Materials and Methods

Mice:

C57BL/6 aged 8–10 weeks were purchased from The Jackson Laboratory (Bar Harbor, ME). S1PR1 flox x Rosa26-Cre-ERT2 (backcrossed with C57BL/6 for 8 generations) (7), S1PR1-Tg mice (backcrossed with C57BL/6 for 8 generations) (34), $S1PR1^{S5A/S5A}$ mice (backcrossed with C57BL/6 for 5 generations) (7) *),* S1PR1 flox x UBC-Cre-ERT2 (C57BL/6 for both S1PR1 and UBC-CreERT2 (51, 52), $S1PR2^{-/-}$ (53), $S1PR4^{-/-}$ (54), $SphK1^{-/-}$ and $SphK2^{-/-}$ (37), were used. All experiments were performed with age- and sex-matched mice and approved by Institutional Animal Care and Utilization Committee at University of Maryland At Baltimore.

Cell lines and primary cells:

SVEC4–10 (designated as SVEC) (CRL-2181) were from the American Type Culture Collection (Manassas, VA). C57BL/6 mouse skin primary LEC and human skin primary LEC were purchased from Cell Biologics (Chicago, IL), and were cultured according to manufacturer's instructions. Human Teff, iTreg and nTreg were generated as previously published (55). Mouse CD4 from spleen and lymph nodes were prepared according to manufacturer's protocols (CD4 enrichment kit, STEMCELL Technologies, Inc., Vancouver, Canada). Naive CD4 ($CD4^+CD44^{low}$) were activated with plate-bound anti-CD3 (pre-coated plate with 5 μg/ml anti-CD3 antibody overnight), 1 μg/ml anti-CD28 and 10 ng/ml IL-2 for 3 days. Naïve, nTreg ($CD4^+CD25^{hi}$), activated CD4 T cells ($CD4^+CD69^+$), and memory CD4 T cells ($CD4^+CD44^{hi}$) were isolated with flow cytometry sorting(27, 29).

Reagents:

S1P was from Avanti polar lipids (Alabaster, AL). Recombinant murine CCL2, CCL5, CCL19, CCL21, CCL22, CXCL10, CXCL12, IL-6, and TNFα were from R&D Systems (Minneapolis, MN). S1PR antagonists W146 (S1PR1), JTE013 (S1PR2), CYM 50358 hydrochloride (S1PR4), ERK inhibitor U0126, sphingosine kinase (Sphk) inhibitor Ski II, ROCK selective inhibitor Y-27632 and Rho selective inhibitor Rhosin were purchased from Tocris (Bristol, UK). Carboxyfluorescein diacetate succinimidyl ester (CFSE) and efluor670

were purchased from Molecular Probes (Eugene, OR). VCAM-1-Ig and ICAM-1-Ig were purchased from Sino Biological (Beijing, China). Anti-S1P mAb (clone LT1002) was kindly supplied by Dr. Roger A. Sabbadini (Lpath, Inc., San Diego, CA). All of the antibodies resources are indicated in Table S1.

In vitro migration:

7.5×10^4 SVEC cells or 15×10^4 primary mLEC and hLEC were seeded on the upper surface of a 5 μm pore size transwell insert coated with 0.2% (wt/vol) gelatin and cultured as described previously (21). For VCAM-1-Ig coating experiments, transwell inserts were coated with 5 μg/ml of VCAM-1-Ig for 2 hours at 37°C. A total of 2×10^5 freshly isolated CD4 T cells were added in a volume of 100 μl (for flow conditions 340 μl) to the upper chambers of a 24-well transwell plate with a 5μm insert (Corning International, Corning, NY). Lower wells contained various concentrations of chemokines: 53 nM CCL19, 42 nM CCL21, 12.5 nM CXCL12, 50 nM IL6, 25.3 nM CCL5, 23.5 nM CCL2, 100 nM S1P or 18.2 nM CCL22 in 600μl (for flow conditions 360 μl) of migration medium (RPMI 1640/0.5% fatty acid-free BSA (Sigma-Aldrich)). The number of T cells that migrated to the lower well after 4 hours was counted with a hemocytometer. The percentage of migrated cells was calculated as the total number of transmigrated cells divided by the total cell input.

Real-time imaging:

20×10^3 CFSE-labeled CD4 T cells in 100 μl migration medium were loaded into the upper chamber of transwell inserts coated with or without SVEC cell layers, then migrated toward 53 nM CCL19 or 100nM S1P. CD4 T cells migrating across LEC were visualized by EVOS™ FL Auto Imaging System (Life Technologies, Carlsbad, CA) with a 20× objective. One image was captured every 5 minutes for 2 hours. Distance from origin, velocity, displacement, and individual cell tracking times were analyzed with Volocity version 6.1.1 (Perkin Elmer).

Footpad migration assay:

As previously described (6), 2×10^6 CFSE labeled CD4 (treated with/without 10 μM S1PR antagonist or 10 μM S1PR4 antagonist) in 30 μl PBS were injected into the footpads that were treated with/without0.5 nM S1PR2 antagonist. For endogenous T cell migration, mice were pretreated with 100 μg anti-CD62L (MEL-14, BioXCell, West Lebanon, NH) i.v., 24 hours later footpads treated with 0.5 nM S1PR2 antagonist, and dLN assessed 16 hours later (29). For LPS (Sigma-Aldrich, St. Louis, MO) induced inflammation, 1 μg LPS in 20 μl PBS was injected per footpad 2 hours prior to T cell transfer. CFSE-labeled CD4 T cells in 30 μl PBS were mixed with 1 μg mouse control IgG or anti-S1P, or 1 μg rat control IgG or anti-VCAM-1, and injected into the footpads. In the paired analysis for footpad migration, T cells are transferred to both hind footpads of a recipient mouse. T cells on one side are treated with active reagent (e.g., receptor blocker), while T cells on the other side are treated with vehicle or control compound. Each mouse thus acts as its own control. Two or 16 hours after injection, mice were euthanized, the draining popliteal lymph nodes (LN) were harvested, and single cell suspensions or tissue sections prepared for flow cytometric or immunohistochemical analysis, respectively.

Whole mount staining of mouse ear pinnae:

1×10^6 CFSE labeled naïve CD4 T cells treated with/without S1PRs antagonists (10 μM S1PR antagonist or 10 μM S1PR4 antagonist) in 10 μl PBS were injected into mouse ear pinnae treated with/without 0.5 nM S1PR2 antagonists or 10 μg/ml anti-CCR7 (in 10 μl PBS) intradermally. 12 hours later, ears were collected and peeled into two halves, fixed with 3% paraformaldehyde (PFA) in PBS for 5 minutes at 4^oC, permeabilized with 1% Triton X in PBS for 30 minutes at 4^oC, incubated with 5% donkey serum (Jackson ImmunoResearch, West Grove, PA) for 30 minutes at 4^oC, and incubated with the primary antibody at 4^oC overnight. The ears were then washed with PBS, incubated with secondary antibody for 4 hours at 4^oC, washed with PBS, and fixed with 3% PFA at 4^oC for 10 minutes. For S1P staining, mouse ears were fixed with 10% buffered formalin for 2 minutes, permeabilized with 0.1% Triton X-100 for 10 minutes, blocked with 2% casein (Sigma-Aldrich, St. Louis, MO) solution in PBS for 10 minutes at room temperature; incubated with anti-S1P (Lpath Inc., San Diego, CA), anti-Lyve-1 for 1 hour at room temperature; then washed and incubated with secondary antibody (donkey anti-rabbit Cy3 at 5 μg/ml (Jackson ImmunoResearch, cat. no. 711–165-152) and donkey anti-mouse Alexa Fluor 488 at 5 μg/ml (Jackson ImmunoResearch, cat. no. 705–546-147) for 1 hour at room temperature. The stained ears were analyzed by fluorescence microscopy (Nikon Eclipse E800, Nikon Co., Tokyo, Japan). For 3-D confocal microscopy, ear pinna samples were visualized with a Zeiss LSM5 Duo with a × 63 or × 40 objective, respectively. Z-stack images were acquired every 1 μm with 10–16 μm slice thicknesses.

Fluorescent flow cytometry:

SVEC and mLEC were treated with various conditions and stained with indicated antibodies. Samples were analyzed with an LSR Fortessa Cell Analyzer (BD Biosciences, San Diego, CA). For apoptosis assays, cells were stained with the 7-AAD and Annexin V apoptosis kit (BD PharMingen, San Diego, CA) according to the manufacturer's protocols and analyzed by flow cytometry. Data were analyzed with FlowJo software v 8.8.7 (Tree Star, Ashland, OR).

Immunofluorescent staining:

SVEC monolayers were stained with anti-VCAM-1, anti-ZO-1 or anti-VE-cadherin for 1 h at 4 °C, then incubated with FITC or Cy3 labeled donkey anti-rat secondary antibody (Jackson ImmunoResearch, West Grove, PA) for 30 min at 4 °C. The inserts were washed with PBS, and fixed with 3% PFA at 4 °C for 10 minutes. The insert membranes were removed from transwell and mounted on slides. For paracellular and transcellular migration, SVEC cells were stained with efluor670 (Molecular Probes, Eugene, OR), then CFSE-labeled CD4 T cells migrated toward CCL19 or S1P across the iSVEC layers. 1h later, the inserts were washed with PBS, and fixed with 3% PFA at 4 °C for 10 minutes, permeabilized with 0.1% Triton-X-100 in PBS for 5 minutes at 4 °C, stained with Alexa Flour 555 labeled phalloidin for 30 minutes at 4 °C. Fluorescence microscopy was performed with aNikon Eclipse E800. 3-D confocal microscopy was performed on cell layers as noted above for ear pinna microscopy with a 63× objective. Quantitative analysis was performed with Volocity 3D Image Analysis Software to demonstrate the distribution of

different molecules on cells, and measure the density of different stains (PerkinElmer, Waltham, MA).

Permeability assays:

For in vitro permeability, iSVEC inserts were pretreated with various conditions noted in the text and figure legends, and 100 μL 0.67 mg/mL Evans Blue (Sigma-Aldrich) in migration medium added to the top chamber and 600 μL migration medium (21) without phenol red was added to the lower chamber. After 0.5, 1, 2, and 3 hours, lower chamber medium was collected, and the optical density at 620 nm was measured in a microplate reader (TECAN, San Jose, CA). For in vivo permeability, vehicle or the S1PR2 antagonist were injected into hind footpads, 1 hour later 30 μL 0.67 mg/mL Evans Blue in PBS was administered in the footpad, and 16 hours later the popliteal dLNs were collected, dissociated in 100 μL PBS, and O.D. 620 measured in a microplate reader.

Lentivirus and infections:

Viruses were packaged target cells infected according to established protocols (56). S1PR1 and S1PR2 shRNAs were purchased from Sigma-Aldrich (St. Louis, MO). Lentiviral particles were produced by cotransfecting HEK293T cells with shRNA plasmid, pCMV-ΔR8.2 packaging plasmid (Addgene, Cambridge, MA), and pCMV-VSVg envelope plasmid (Addgene)For infection, lentivirus preparations were mixed with 6 μg/ml polybrene (American Bioanalytical, Natick, MA) and applied to SVEC at an MOI of 2. Knockdown of S1PR expression was analyzed by RT-PCR, and the cells used for in vitro migration assays.

Western Blotting:

1×10^6 cells were lysed with buffer containing 20 mM HEPES, pH 7.4, 1% Triton X-100, 150 mM NaCl, 12.5 mM β-glycerophosphate, 50 mM NaF, 1 mM DTT, 1 mM sodium orthovanadate, 2 mM EDTA, 1 mM PMSF, and protease inhibitor mixture (Roche Applied Science). Protein concentrations were measured with the Quick Start™ Bradford Protein Assay (BioRad, Philadelphia, PA) and equal amount of proteins were loaded and separated on 4–20% mini-gels (Invitrogen), electrotransferred to Immobilon-P membranes (Millipore, Darmstadt, Germany), blocked, and probed with the indicated antibodies.

Statistical Analysis:

In vitro transwell migration assays were performed at least three times for individual experiments, and results represent mean values of triplicate samples. In vivo migration experiments were performed at least two times to collect enough data points to perform statistical analysis, usually 6–15 mice/group. Immunohistochemistry and H&E staining were performed at least three times for individual experiments (2 inserts/experiment), and 10 fields/insert acquired. All flow cytometry experiments were performed at least three times. Fluorescence images were analyzed with Velocity software for quantification of fluorescence density. Other results were analyzed by GraphPad Prism Software (version 5, GraphPad Software, Inc., La Jolla, CA) and presented as the mean ± SEM. Statistical analyses were performed using Student's t test. One-way ANOVA was used for multiple comparisons. $P < 0.05$ was considered statistically significant. No statistical tests were used

to predetermine the size of experiments. Sample and experiment sizes were determined empirically for sufficient statistical power. No samples were excluded specifically from analysis, and no randomization or blinding protocol was used.

Supplementary Material

Refer to Web version on PubMed Central for supplementary material.

Acknowledgments:

We thank performed at the University of Maryland Marlene and Stewart Greenebaum Cancer Center Flow Cytometry Shared Service.

Funding: Supported by R01AI062765, AI114496 to JSB; Division of Intramural Research Programs, NIAID to AO; R35 HL135821 to TH; RO1 HL11879 to BRB; and R01AI085166, R01AI123308 to SRS.

References and notes

1. Matloubian M et al., Lymphocyte egress from thymus and peripheral lymphoid organs is dependent on S1P receptor 1. Nature 427, 355 (1 22, 2004). [PubMed: 14737169]
2. Pham TH, Okada T, Matloubian M, Lo CG, Cyster JG, S1P1 receptor signaling overrides retention mediated by G alpha i-coupled receptors to promote T cell egress. Immunity 28, 122 (1, 2008). [PubMed: 18164221]
3. Grigorova IL et al., Cortical sinus probing, S1P1-dependent entry and flow-based capture of egressing T cells. Nature immunology 10, 58 (1, 2009). [PubMed: 19060900]
4. Brinkmann V, Cyster JG, Hla T, FTY720: sphingosine 1-phosphate receptor-1 in the control of lymphocyte egress and endothelial barrier function. American journal of transplantation : official journal of the American Society of Transplantation and the American Society of Transplant Surgeons 4, 1019 (7, 2004).
5. Wei SH et al., Sphingosine 1-phosphate type 1 receptor agonism inhibits transendothelial migration of medullary T cells to lymphatic sinuses. Nature immunology 6, 1228 (12, 2005). [PubMed: 16273098]
6. Ledgerwood LG et al., The sphingosine 1-phosphate receptor 1 causes tissue retention by inhibiting the entry of peripheral tissue T lymphocytes into afferent lymphatics. Nature immunology 9, 42 (1, 2008). [PubMed: 18037890]
7. Jung B et al., Flow-regulated endothelial S1P receptor-1 signaling sustains vascular development. Developmental cell 23, 600 (9 11, 2012). [PubMed: 22975328]
8. Lee MJ et al., Vascular endothelial cell adherens junction assembly and morphogenesis induced by sphingosine-1-phosphate. Cell 99, 301 (10 29, 1999). [PubMed: 10555146]
9. Kimura T et al., Sphingosine 1-phosphate stimulates proliferation and migration of human endothelial cells possibly through the lipid receptors, Edg-1 and Edg-3. The Biochemical journal 348 Pt 1, 71 (5 15, 2000). [PubMed: 10794715]
10. Gaengel K et al., The sphingosine-1-phosphate receptor S1PR1 restricts sprouting angiogenesis by regulating the interplay between VE-cadherin and VEGFR2. Developmental cell 23, 587 (9 11, 2012). [PubMed: 22975327]
11. Sanchez T et al., Phosphorylation and action of the immunomodulator FTY720 inhibits vascular endothelial cell growth factor-induced vascular permeability. The Journal of biological chemistry 278, 47281 (11 21, 2003). [PubMed: 12954648]
12. Yanagida K et al., Size-selective opening of the blood-brain barrier by targeting endothelial sphingosine 1-phosphate receptor 1. Proceedings of the National Academy of Sciences of the United States of America 114, 4531 (4 25, 2017). [PubMed: 28396408]
13. Cyster JG, Schwab SR, Sphingosine-1-phosphate and lymphocyte egress from lymphoid organs. Annual review of immunology 30, 69 (2012).

14. Cinamon G et al., Sphingosine 1-phosphate receptor 1 promotes B cell localization in the splenic marginal zone. Nature immunology 5, 713 (7, 2004). [PubMed: 15184895]
15. Allende ML et al., S1P1 receptor directs the release of immature B cells from bone marrow into blood. The Journal of experimental medicine 207, 1113 (5 10, 2010). [PubMed: 20404103]
16. Sic H et al., Sphingosine-1-phosphate receptors control B-cell migration through signaling components associated with primary immunodeficiencies, chronic lymphocytic leukemia, and multiple sclerosis. The Journal of allergy and clinical immunology 134, 420 (8, 2014). [PubMed: 24679343]
17. Singer II et al., Sphingosine-1-phosphate agonists increase macrophage homing, lymphocyte contacts, and endothelial junctional complex formation in murine lymph nodes. J Immunol 175, 7151 (12 1, 2005). [PubMed: 16301618]
18. Czeloth N, Bernhardt G, Hofmann F, Genth H, Forster R, Sphingosine-1-phosphate mediates migration of mature dendritic cells. J Immunol 175, 2960 (9 1, 2005). [PubMed: 16116182]
19. Lamana A et al., CD69 modulates sphingosine-1-phosphate-induced migration of skin dendritic cells. The Journal of investigative dermatology 131, 1503 (7, 2011). [PubMed: 21412255]
20. Huang Y et al., S1P-dependent interorgan trafficking of group 2 innate lymphoid cells supports host defense. Science 359, 114 (1 5, 2018). [PubMed: 29302015]
21. Xiong Y et al., A robust in vitro model for trans-lymphatic endothelial migration. Scientific reports 7, 1633 (5 9, 2017). [PubMed: 28487567]
22. Kabashima K et al., Plasma cell S1P1 expression determines secondary lymphoid organ retention versus bone marrow tropism. The Journal of experimental medicine 203, 2683 (11 27, 2006). [PubMed: 17101733]
23. Vaahtomeri K et al., Locally Triggered Release of the Chemokine CCL21 Promotes Dendritic Cell Transmigration across Lymphatic Endothelia. Cell reports 19, 902 (5 02, 2017). [PubMed: 28467903]
24. Tal O et al., DC mobilization from the skin requires docking to immobilized CCL21 on lymphatic endothelium and intralymphatic crawling. The Journal of experimental medicine 208, 2141 (9 26, 2011). [PubMed: 21930767]
25. Weber M et al., Interstitial dendritic cell guidance by haptotactic chemokine gradients. Science 339, 328 (1 18, 2013). [PubMed: 23329049]
26. Johnson LA et al., An inflammation-induced mechanism for leukocyte transmigration across lymphatic vessel endothelium. The Journal of experimental medicine 203, 2763 (11 27, 2006). [PubMed: 17116732]
27. Brinkman CC et al., Treg engage lymphotoxin beta receptor for afferent lymphatic transendothelial migration. Nature communications 7, 12021 (6 21, 2016).
28. Haessler U, Teo JC, Foretay D, Renaud P, Swartz MA, Migration dynamics of breast cancer cells in a tunable 3D interstitial flow chamber. Integrative biology : quantitative biosciences from nano to macro 4, 401 (4, 2012). [PubMed: 22143066]
29. Xiong Y, Ahmad S, Iwami D, Brinkman CC, Bromberg JS, T-bet Regulates Natural Regulatory T Cell Afferent Lymphatic Migration and Suppressive Function. J Immunol 196, 2526 (3 15, 2016). [PubMed: 26880765]
30. Zhang G et al., Critical role of sphingosine-1-phosphate receptor 2 (S1PR2) in acute vascular inflammation. Blood 122, 443 (7 18, 2013). [PubMed: 23723450]
31. Mendoza A et al., Lymphatic endothelial S1P promotes mitochondrial function and survival in naive T cells. Nature 546, 158 (6 1, 2017). [PubMed: 28538737]
32. Sanna MG et al., Enhancement of capillary leakage and restoration of lymphocyte egress by a chiral S1P1 antagonist in vivo. Nature chemical biology 2, 434 (8, 2006). [PubMed: 16829954]
33. Guerrero M et al., Discovery, design and synthesis of the first reported potent and selective sphingosine-1-phosphate 4 (S1P4) receptor antagonists. Bioorganic & medicinal chemistry letters 21, 3632 (6 15, 2011). [PubMed: 21570287]
34. Thangada S et al., Cell-surface residence of sphingosine 1-phosphate receptor 1 on lymphocytes determines lymphocyte egress kinetics. The Journal of experimental medicine 207, 1475 (7 5, 2010). [PubMed: 20584883]

35. Gomez D, Diehl MC, Crosby EJ, Weinkopff T, Debes GF, Effector T Cell Egress via Afferent Lymph Modulates Local Tissue Inflammation. J Immunol 195, 3531 (10 15, 2015). [PubMed: 26355150]
36. Teijeira A et al., T Cell Migration from Inflamed Skin to Draining Lymph Nodes Requires Intralymphatic Crawling Supported by ICAM-1/LFA-1 Interactions. Cell reports 18, 857 (1 24, 2017). [PubMed: 28122237]
37. Allende ML et al., Mice deficient in sphingosine kinase 1 are rendered lymphopenic by FTY720. The Journal of biological chemistry 279, 52487 (12 10, 2004). [PubMed: 15459201]
38. Sanchez T et al., Induction of vascular permeability by the sphingosine-1-phosphate receptor-2 (S1P2R) and its downstream effectors ROCK and PTEN. Arteriosclerosis, thrombosis, and vascular biology 27, 1312 (6, 2007).
39. Pham TH et al., Lymphatic endothelial cell sphingosine kinase activity is required for lymphocyte egress and lymphatic patterning. The Journal of experimental medicine 207, 17 (1 18, 2010). [PubMed: 20026661]
40. Baluk P et al., Functionally specialized junctions between endothelial cells of lymphatic vessels. The Journal of experimental medicine 204, 2349 (10 1, 2007). [PubMed: 17846148]
41. Pflicke H, Sixt M, Preformed portals facilitate dendritic cell entry into afferent lymphatic vessels. The Journal of experimental medicine 206, 2925 (12 21, 2009). [PubMed: 19995949]
42. Mamdouh Z, Mikhailov A, Muller WA, Transcellular migration of leukocytes is mediated by the endothelial lateral border recycling compartment. The Journal of experimental medicine 206, 2795 (11 23, 2009). [PubMed: 19887395]
43. Muller WA, Transendothelial migration: unifying principles from the endothelial perspective. Immunological reviews 273, 61 (9, 2016). [PubMed: 27558328]
44. Zhang W et al., Sphingosine-1-phosphate receptor-2 mediated NFkappaB activation contributes to tumor necrosis factor-alpha induced VCAM-1 and ICAM-1 expression in endothelial cells. Prostaglandins & other lipid mediators 106, 62 (10, 2013). [PubMed: 23770055]
45. Barreiro O et al., Dynamic interaction of VCAM-1 and ICAM-1 with moesin and ezrin in a novel endothelial docking structure for adherent leukocytes. The Journal of cell biology 157, 1233 (6 24, 2002). [PubMed: 12082081]
46. Carman CV, Springer TA, A transmigratory cup in leukocyte diapedesis both through individual vascular endothelial cells and between them. The Journal of cell biology 167, 377 (10 25, 2004). [PubMed: 15504916]
47. Russo E et al., Intralymphatic CCL21 Promotes Tissue Egress of Dendritic Cells through Afferent Lymphatic Vessels. Cell reports 14, 1723 (2 23, 2016). [PubMed: 26876174]
48. Drouillard A et al., Human Naive and Memory T Cells Display Opposite Migratory Responses to Sphingosine-1 Phosphate. J Immunol 200, 551 (1 15, 2018). [PubMed: 29237776]
49. Xiong Y, Hla T, S1P control of endothelial integrity. Current topics in microbiology and immunology 378, 85 (2014). [PubMed: 24728594]
50. Hagerling R et al., Distinct roles of VE-cadherin for development and maintenance of specific lymph vessel beds. The EMBO journal 37, (11 15, 2018).
51. Ruzankina Y et al., Deletion of the developmentally essential gene ATR in adult mice leads to age-related phenotypes and stem cell loss. Cell stem cell 1, 113 (6 7, 2007). [PubMed: 18371340]
52. Allende ML, Yamashita T, Proia RL, G-protein-coupled receptor S1P1 acts within endothelial cells to regulate vascular maturation. Blood 102, 3665 (11 15, 2003). [PubMed: 12869509]
53. Skoura A et al., Essential role of sphingosine 1-phosphate receptor 2 in pathological angiogenesis of the mouse retina. The Journal of clinical investigation 117, 2506 (9, 2007). [PubMed: 17710232]
54. Allende ML et al., Sphingosine-1-phosphate lyase deficiency produces a pro-inflammatory response while impairing neutrophil trafficking. The Journal of biological chemistry 286, 7348 (3 4, 2011). [PubMed: 21173151]
55. Lu Y et al., miR-146b antagomir-treated human Tregs acquire increased GVHD inhibitory potency. Blood 128, 1424 (9 8, 2016). [PubMed: 27485827]

56. Driesbaugh KH et al., Proteolytic activation of the protease-activated receptor (PAR)-2 by the glycosylphosphatidylinositol-anchored serine protease testisin. The Journal of biological chemistry 290, 3529 (2 6, 2015). [PubMed: 25519908]

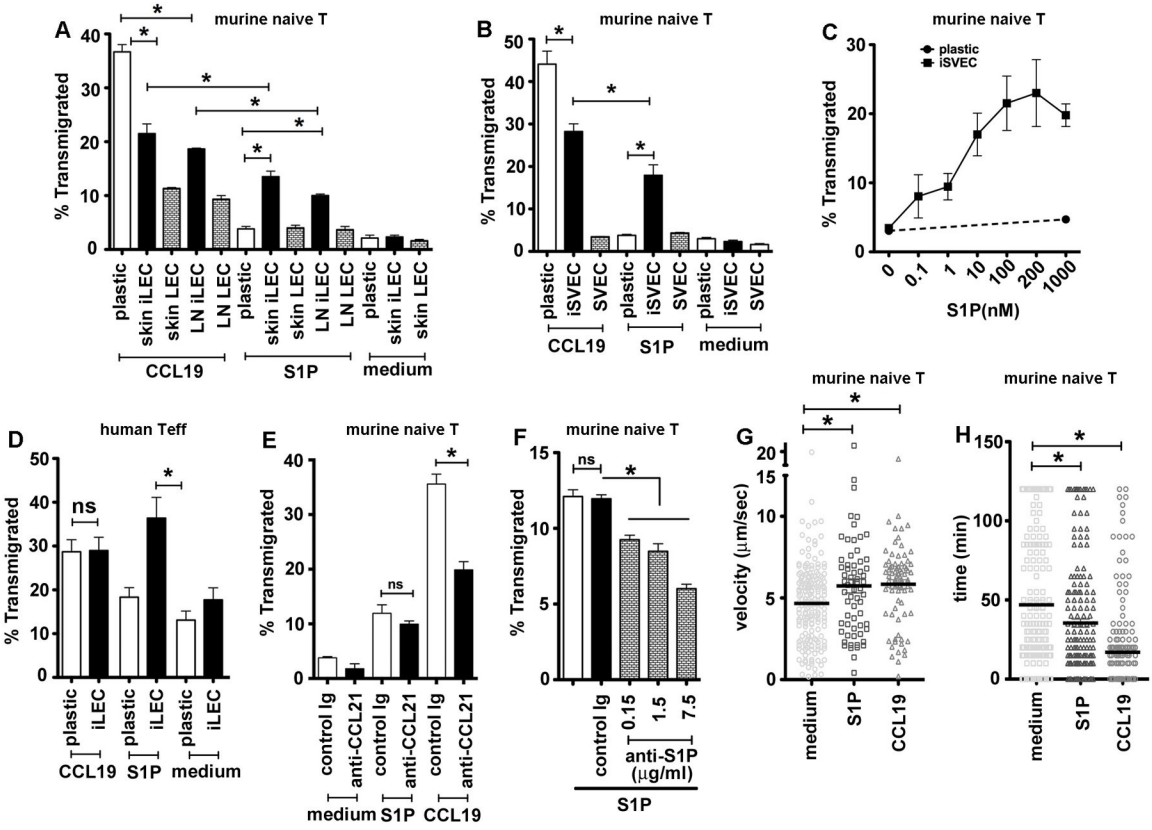

Fig. 1. LEC specifically promote CD4 T cell TEM to S1P but not other chemokines.

Murine CD4 migration: (A) across plastic, or skin or LN derived iLEC or LEC, to S1P or CCL19; (B) across plastic, iSVEC or SVEC to medium, 100 nM S1P or 53 nM CCL19; (C) across plastic or iSVEC to varying doses of S1P. (D) Migration of human Teff across plastic, human iLEC or human LEC to CCL19, or S1P. (E) Naïve murine CD4 migration toward S1P or CCL19 across iSVEC, with anti-CCL21 loaded in the upper chamber. (F) Naïve murine CD4 migration across iSVEC toward S1P with various doses of anti-S1P in the upper chamber. (G-H) Individual naïve CD4 migration toward S1P and CCL19, showing velocity (G) and migration time (H) of individual cells. At least three independent experiments, triplicate wells. Data presented as mean ± SEM. One-way ANOVA for multiple comparisons. *$p < 0.05$; ns, not significant.

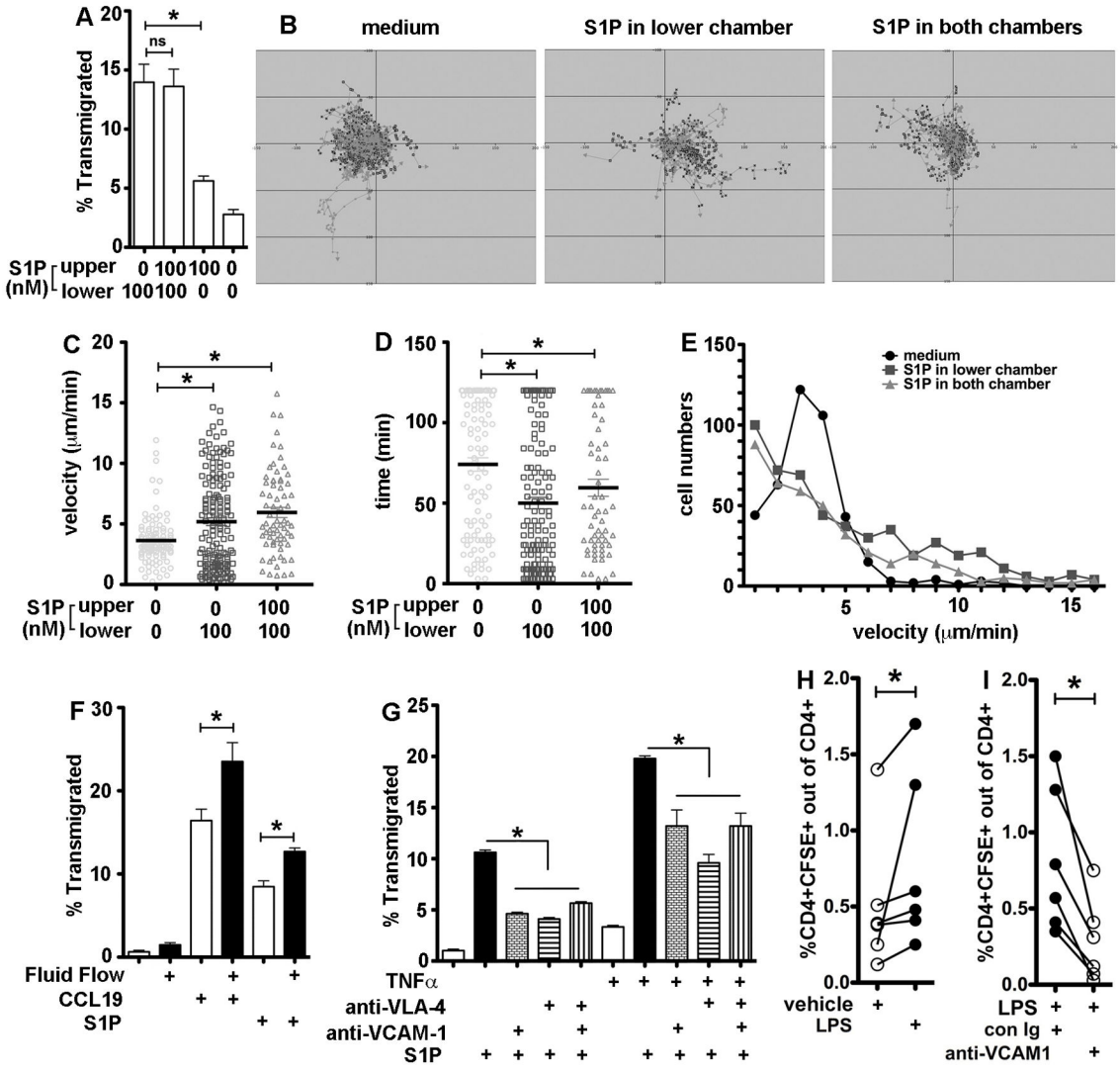

Fig. 2. S1P induces T cell chemotactic and chemokinetic TEM regulated by fluid flow and inflammation.

(A) Naïve CD4 migration across iSVEC; S1P loaded in different chambers as indicated. (B-E) Real-time imaging for naïve CD4 chemokinetic or chemotactic migration toward S1P loaded in the lower or both chambers, respectively. (B) Tracking for individual cells, (C) velocity, (D) migration times and (E) velocity distribution. (F) Naïve CD4 migration across iSVEC to CCL19 or S1P under no flow or flow conditions. (G) Migration of naive CD4 pretreated with or without anti-VLA-4 to S1P across iSVEC pretreated with anti-VCAM-1 and/or TNFα 3 hours prior to anti-VCAM-1. For A-G, three independent experiments with triplicate wells, presented as mean ± SEM; one-way ANOVA for multiple comparisons. (H-I) Footpad migration with or without LPS treatment. 1 μg LPS injected per footpad; 2 hours later CD4 T cells without treatment (H), or mixed with control IgG or anti-VCAM-1 (I), transferred into footpads and migration to dLN assessed after 16 hours (n=6). For H-I, statistical analyses, paired Student's t test, *p< 0.05.

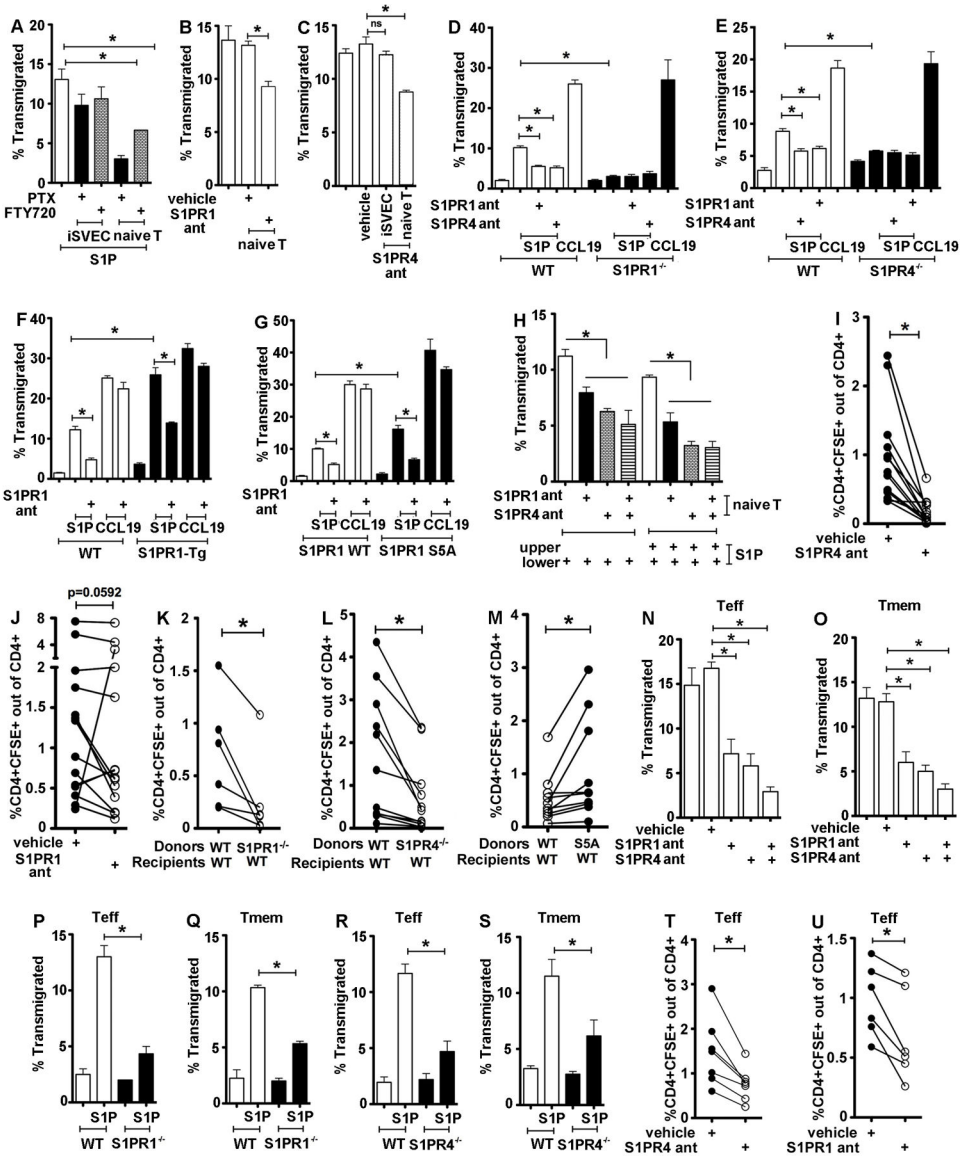

Fig. 3. T cell S1PR1 and S1PR4 regulate TEM.

(A) iSVEC or CD4 treated with PTX, FTY720; (B) CD4 treated with S1PR1 antagonist; (C) iSVEC or CD4 treated with S1PR4 antagonist; (D) $S1PR1^{-/-}$ or $S1PR1^{+/+}$ (WT), (E) $S1PR4^{-/-}$ or $S1PR4^{+/+}$, CD4 treated with S1PR1 or S1PR4 antagonists, migrated to S1P or CCL19. (F) S1PR1-Tg or (G) S1PR1 S5A CD4 treated with S1PR1 antagonist, migrated to S1P, CCL19. (H) CD4 treated with S1PR1, S1PR4 or combined antagonists, iSVEC, S1P in lower or both chambers. (I-M) Naïve CD4 footpad migration: (I) CD4 pretreated with S1PR4 antagonist (n=12); (J) CD4 pretreated with S1PR1 antagonist (n=12); (K) $S1PR1^{+/+}$ or $S1PR1^{-/-}$ CD4 transferred to WT recipients (n=6); (L) $S1PR4^{+/+}$ or $S1PR4^{-/-}$ CD4 to WT recipients (n=12); (M) S1PR1 wild type or S5A CD4 to WT recipients (n=10). (N-S) CD4 Teff or Tmem across iLEC: (N) Teff or (O) Tmem treated with S1PR1, S1PR4 or combined antagonists; $S1PR1^{-/-}$ or $S1PR1^{+/+}$ (P) Teff or (Q) Tmem; $S1PR4^{-/-}$ or $S1PR4^{+/+}$ (R) Teff or (S) Tmem. (T-U) Teff footpad migration: (T) Teff pretreated with S1PR4

antagonist (n=7); or (U) S1PR1 antagonist (n=6). Paired analysis footpad migration, T cells transferred to both footpads, one side treated with inhibitor, other with control. A-H and N-S, mean ± SEM, one-way ANOVA for multiple comparisons. I-M and T-U, paired Student's t test.

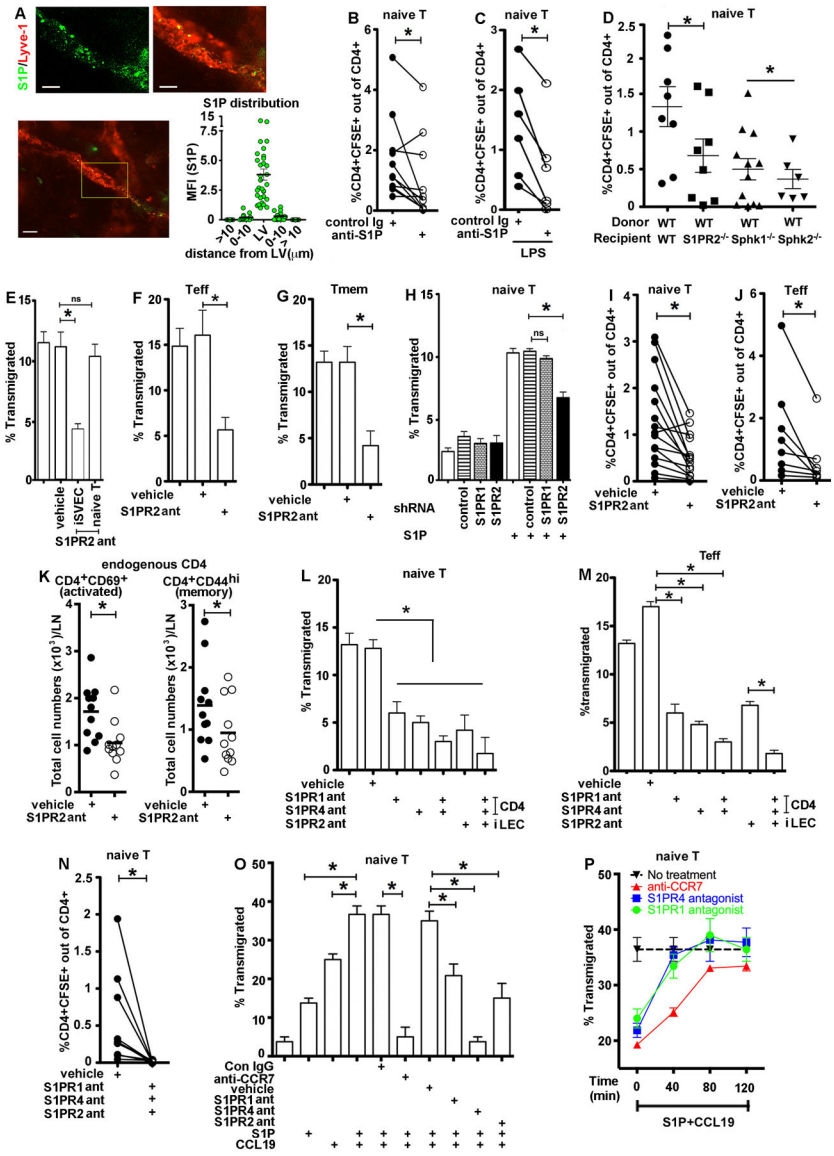

Fig. 4. S1P gradient and LEC S1PR2 regulate T cell TEM.

A) Whole mount staining, S1P in lymphatics. 100x, scale bar 8 μm (2 ears/treatment/experiment, n=8). LV: lymphatic vessel. (B) Naïve CD4, footpad migration, anti-S1P treatment (n=11). (C) Naïve CD4, footpad (treated with LPS) migration, anti-S1P (n=6). (D) Wild type (WT) into WT, S1PR2$^{-/-}$, Sphk1$^{-/-}$ or Sphk2$^{-/-}$ recipients (n=8 WT, S1PR2$^{-/-}$; n=12 Sphk1$^{-/-}$; n=6 Sphk2$^{-/-}$). (E-H) CD4 across iSVEC to S1P: (E) Naïve CD4, (F) Teff and (G) Tmem across iSVEC treated with S1PR2 antagonist. (H) iSVEC infected with shRNA lentivirus. (I-K) CD4 footpad migration: (I) Naive CD4 and (J) Teff, footpads pretreated with S1PR2 antagonist (n=15 naïve, n=8 Teff); (K) Endogenous T cell migration, anti-CD62L mAb i.v. and S1PR2 antagonist in footpad; total CD4^{+}CD69^{+} activated and CD4^{+}CD44^{hi} memory in dLN (n=10). (L-M) CD4 across iLEC to S1P: (L) Naïve CD4 or (M) Teff pretreated with S1PR1, S1PR4, or combined antagonists; iLEC treated with S1PR2 antagonist. (N) Naïve CD4 pretreated with S1PR1 and S1PR4 antagonists into footpad

pretreated with S1PR2 antagonist (n=8). (O) Naïve CD4 treated as indicated; iSVEC treated with S1PR2 antagonist; S1P plus CCL19. (P) Anti-CCR7 or S1PR1 or S1PR4 antagonists added at indicated time points. For E-H, L-M, O-P mean ± SEM, three independent experiments, one-way ANOVA for multiple comparisons; for B, C,, I, J, N paired Student's t test; for K, unpaired Student's t test; for D, Mann-Whitney.

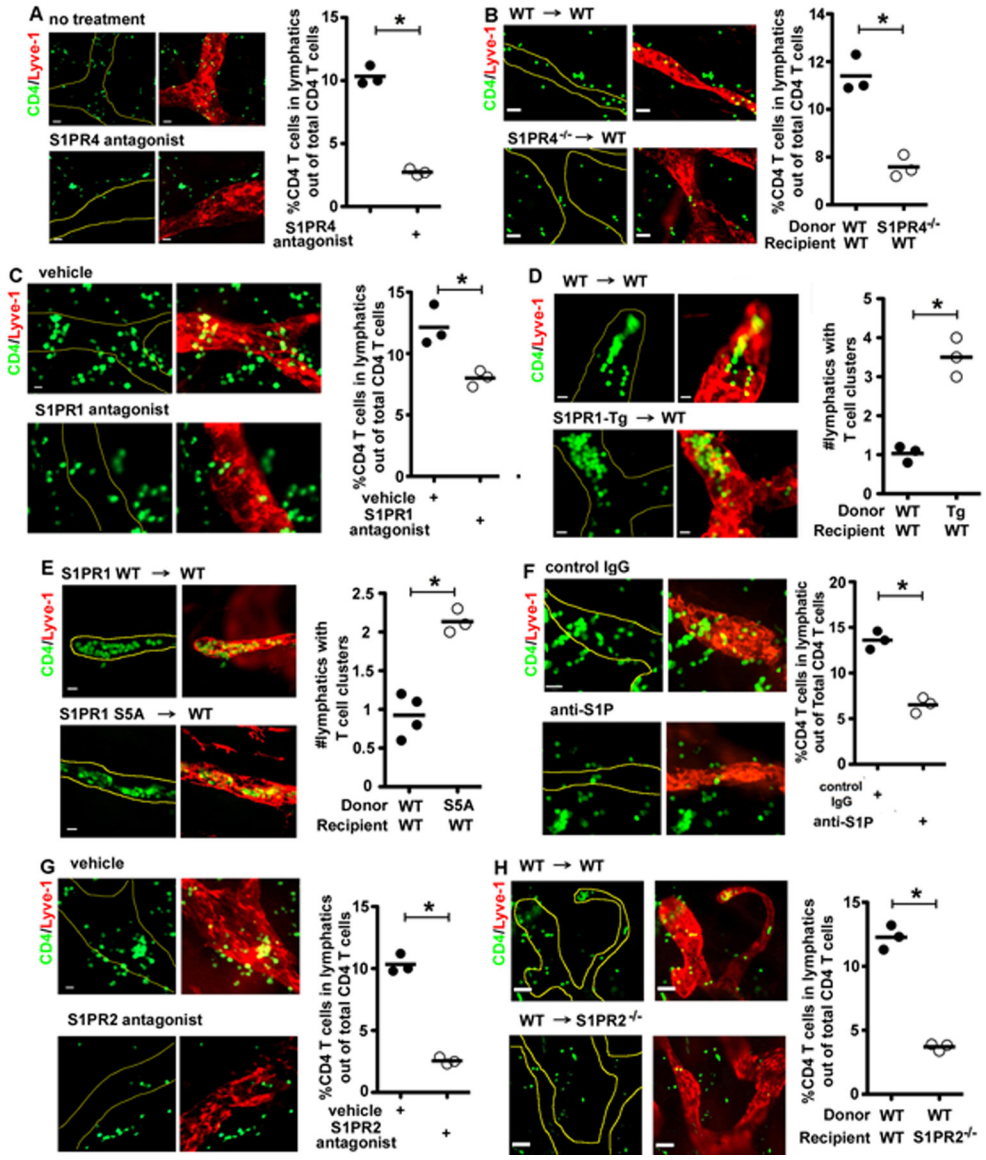

Fig. 5. S1PRs regulate CD4 T cell afferent lymphatic distribution.

Naïve CD4, ear pinnae migration. (A) CD4 treated with S1PR4 antagonist, into pinnae. (B) Wild type (WT) and S1PR4$^{-/-}$ CD4, into wild type pinnae. After 16 hours, pinnae stained for Lyve-1. (C) CD4 treated with S1PR1 antagonist, into pinnae. (D) S1PR1-Tg or (E) S1PR1 S5A or littermate CD4, wild type pinnae. After 2 hours, pinnae stained for Lyve-1. (F) CD4, into pinnae treated with anti-S1P. (G) CD4, into pinnae treated with S1PR2 antagonist; and (H) wild type CD4, into wild type or S1PR2$^{-/-}$ pinnae. After 16 hours, pinnae stained for Lyve-1. Samples analyzed by fluorescence microscopy, magnification 40x, scale bar 8 μm. Percentage of CD4 in lymphatics out of total CD4, or number of lymphatic vessel lumens with clustered groups of CD4, calculated per high-powered field. Four independent experiments, 2 ears/treatment/experiment, 6–8 mice/group, 10 high-powered fields from each pinna. Statistical analyses, Student's t test.

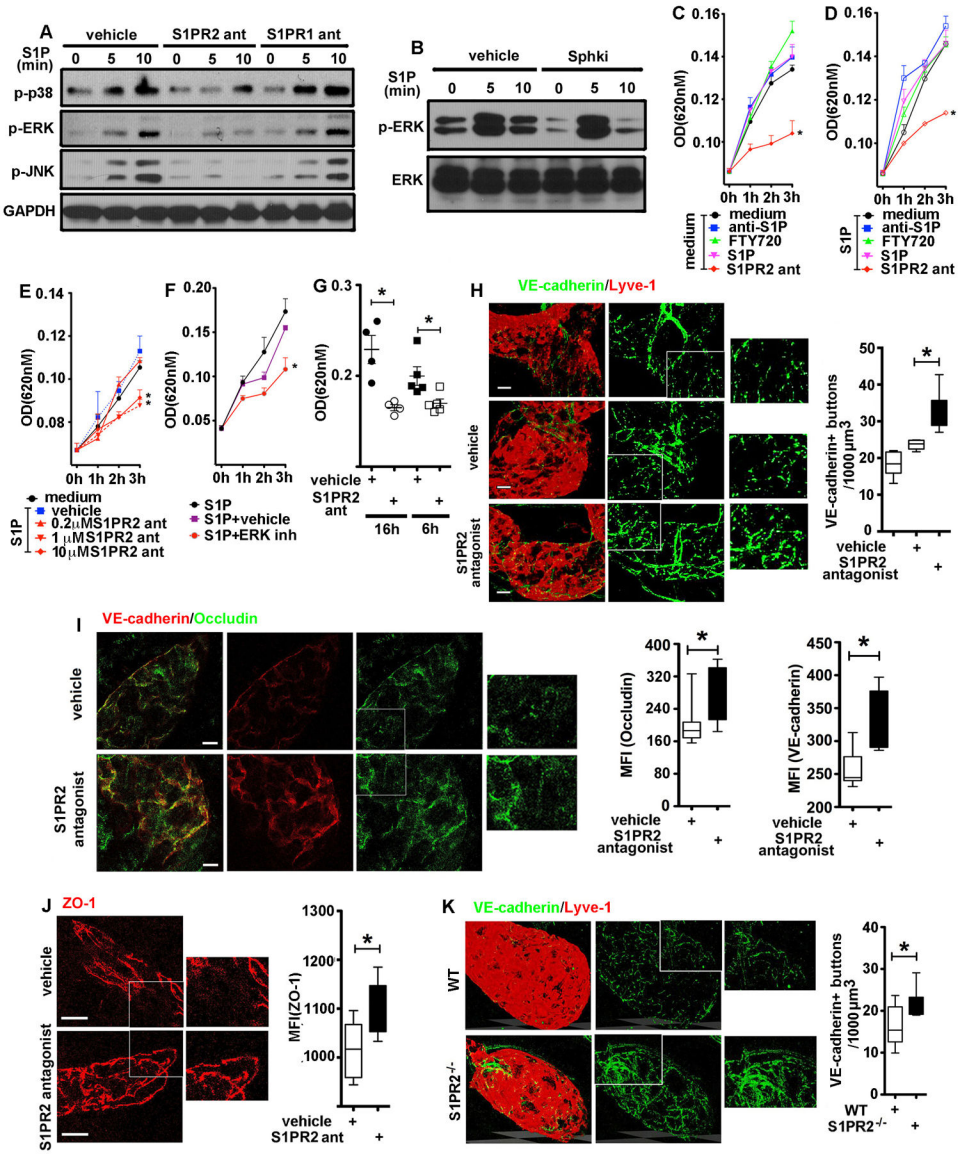

Fig. 6. S1PR2 regulates LEC layer integrity and junction molecules.

(A-B) Western blot: SVEC pretreated with S1PR2 or S1PR1 antagonists, stimulated with S1P (A); SVEC pretreated with Sphki, stimulated with S1P (B). (C-F) Permeability assays: Evans Blue upper chamber; S1P lower chamber; SVEC treated as indicated; three independent experiments. (G) In vivo permeability, footpad treated with S1PR2 antagonist, Evans Blue to dLN measured at indicated times. (H-J) Junction molecule immunohistochemistry: ears treated with S1PR2 antagonist; Lyve-1, VE-cadherin (H); VE-cadherin, occludin (I); ZO-1 (J). (K) VE-cadherin by WT and S1PR2$^{-/-}$ lymphatics (2 ears/treatment/experiment, n=6); magnification 40x, scale bar 21 μm. (L-N) Junction molecule expression, SVEC treated with inhibitors. Mean ± SEM: (C-F; K) one-way ANOVA for multiple comparisons; (G-J) Student's t test.

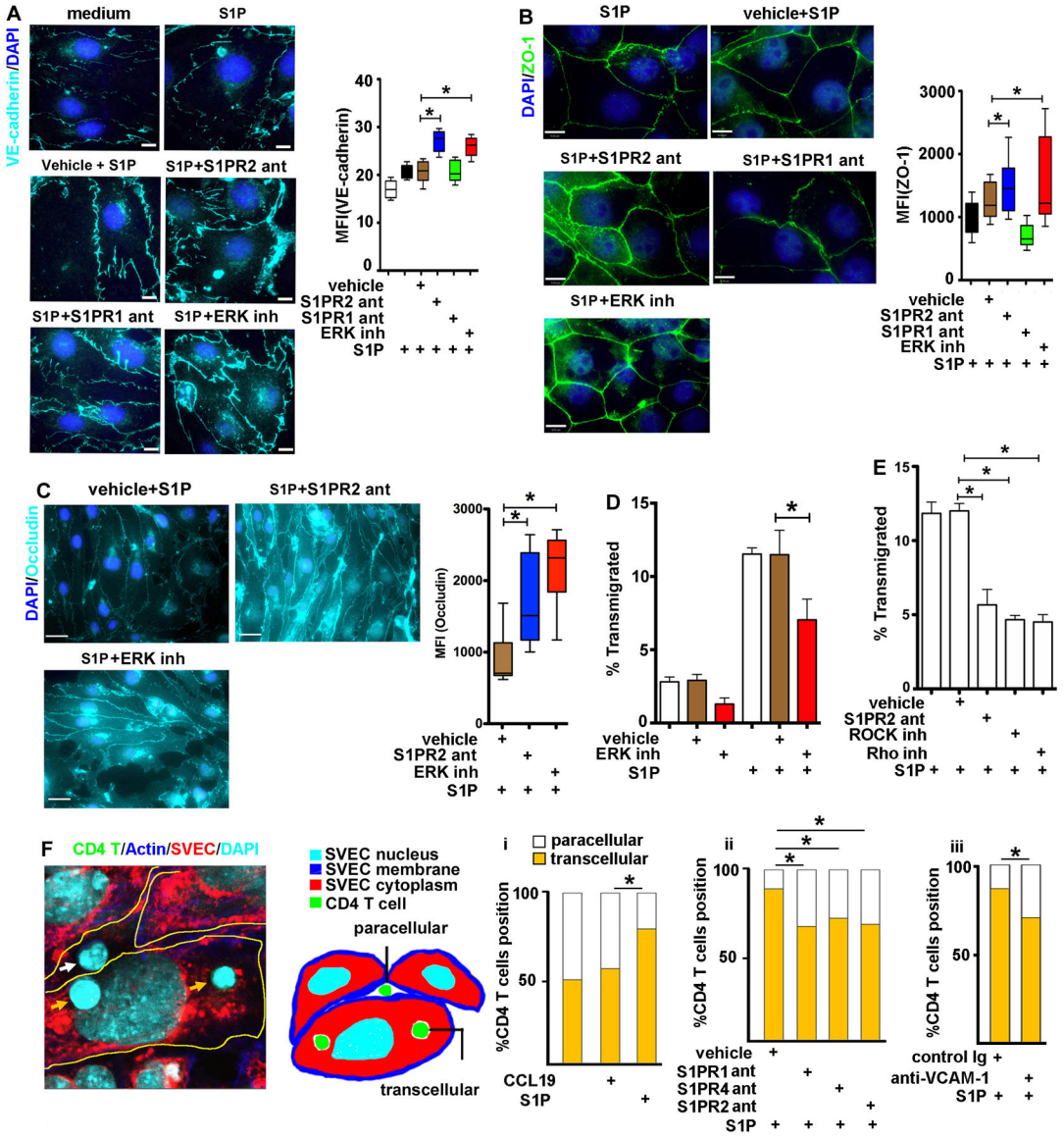

Fig. 7. S1PR2 regulates junction molecules and S1PRs mediates T cells paracellular and transcellular migrations.

(A) VE-cadherin; (B) ZO-1; (C) occludin. SVEC pretreated with S1PR2 or S1PR1 antagonists; ERK inhibitor; stimulated with S1P. Magnification 100x, scale bar 8 μm; three independent experiments. (D) CD4 migration, iSVEC treated with ERK inhibitor, (E) ROCK or Rho inhibitors; three independent experiments. (F) CFSE-labeled CD4, toward S1P and CCL19 (i); T cells pretreated with S1PR1 or S1PR4 antagonists eflour670-labeled SVEC pretreated with S1PR2 antagonist, toward S1P (ii); eflour670-labeled SVEC pretreated with anti-VCAM-1 (iii); magnification 63x, scale bar 14μm; arrowheads indicate paracellular (white) and transcellular (yellow) migration. Percentage of T cells in paracellular and transcellular positions (right); > 159 cells counted/group; three independent experiments. Mean ± SEM: (L-P) one-way ANOVA for multiple comparisons.

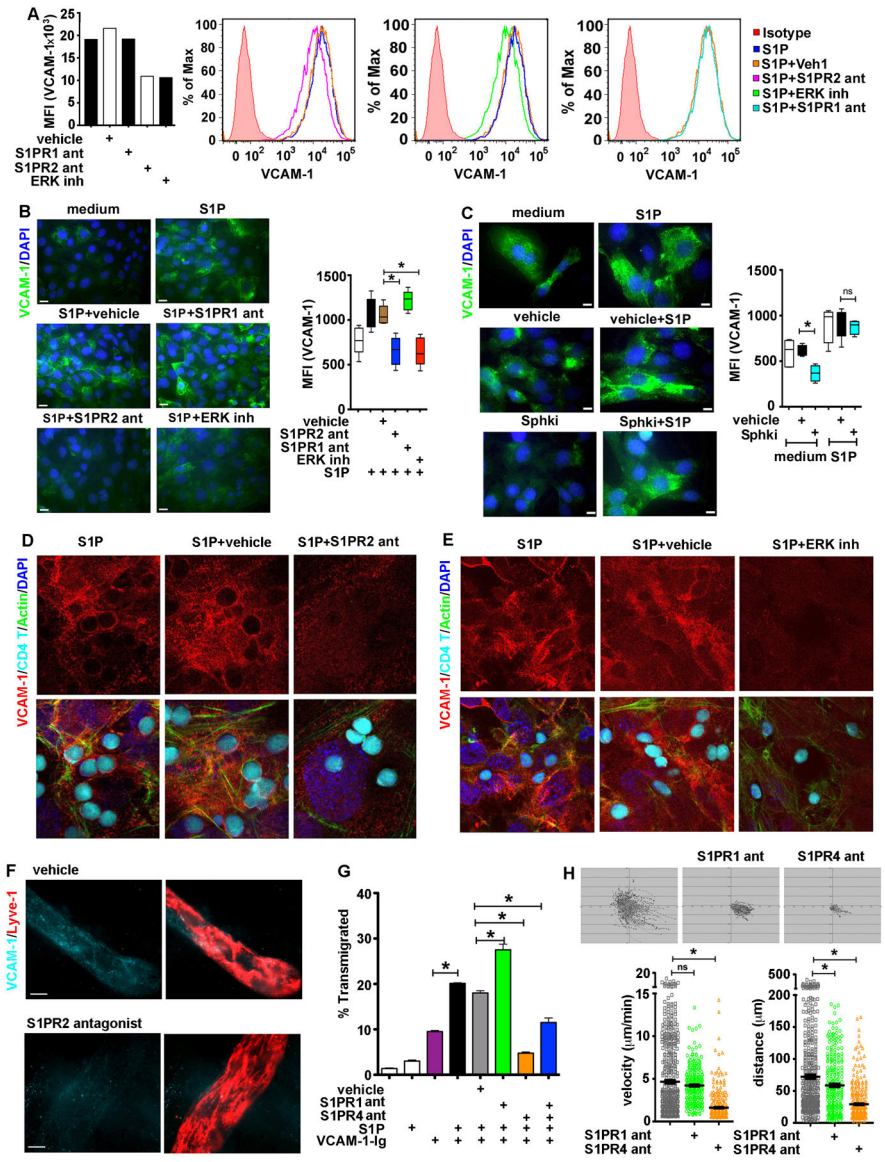

Fig. 8. LEC S1PR2 regulates VCAM-1 expression.

(A) VCAM-1 expression, SVEC treated with S1P, S1PR1 antagonist, S1PR2 antagonist, or ERK inhibitor for 3 hours. Flow cytometry analysis, three independent experiments. (B) VCAM-1 expression, SVEC layers pre-treated with S1PR2 antagonist, S1PR1 antagonist or 5 μM ERK inhibitor, then treated with S1P. Fluorescence microscopy analysis, 40x, scale bar 21 μm. (C) VCAM-1 expression, SVEC pretreated with Sphki, then treated with S1P. Fluorescence microscopy analysis, 100x, scale bar 8 μm. (D-E) CD4 position, LEC VCAM-1 and actin distribution. CD4 migration to S1P for 1 hour over iSVEC pretreated for 1 hour with (D) S1PR2 antagonist, or (E) ERK inhibitor, at least three independent experiments. (F) VCAM-1 expression, afferent lymphatics treated with 0.5 nM S1PR2 antagonist overnight, 40x, scale bar 21 μm. (G) Naïve CD4, treated with S1PR1 or S1PR4 antagonists, migrated to S1P, across transwell inserts coated with VCAM-1-Ig, three independent experiments. (H) Naïve CD4, treated with S1PR1 or S1PR4 antagonists,

migrated to S1P, across transwell inserts coated with VCAM-1-Ig. Real-time imaging, tracking path (left), velocity (middle), distances (right) of individual cells. One-way ANOVA for multiple comparisons (B, C, F and G).